Korean J. Chem. Eng., 34(4), 1081-1090 (2017)
DOI: 10.1007/s11814-017-0015-3

pISSN: 0256-1115
eISSN: 1975-7220

The effects of the thermal treatment of activated carbon on the phenols adsorption

Krzysztof Kuśmierek*,†, Andrzej Świątkowski*, Katarzyna Skrzypczyńska*, Stanisław Błażewicz, and Jakub Hryniewicz***

*Institute of Chemistry, Military University of Technology, Kaliskiego 2, 00-908 Warsaw, Poland
**Faculty of Materials Science and Ceramics, AGH University of Science and Technology, 30-059 Krakow, Poland
(*Received 1 September 2016 • accepted 2 February 2017*)

Abstract−The adsorptive properties of thermally treated activated carbon at 1,500 and 1,800 °C were investigated. The adsorption kinetics and adsorption efficiency of phenol, 4-chlorophenol and 2,4-dichlorophenol from aqueous solutions were examined. The adsorption kinetic data were analyzed using the pseudo-first and pseudo-second order models, while the equilibrium adsorption data were described by the Langmuir and Freundlich isotherms. The adsorption rate and efficiency increased in the order: phenol<4-chlorophenol<2,4-dichlorophenol. The activated carbons were also used for the modification of the carbon paste electrodes for the detection of the phenols based on the differential pulse voltammetry. Compared to the non-modified electrode, all the new paste electrodes showed a significantly greater sensitivity for the detection of the phenols. The signal response was closely related to the porosity of the materials used, and increased with an increase in the adsorption ability and the specific surface area of the modifiers.

Keywords: Activated Carbon, Thermal Treatment, Adsorption, Carbon Paste Electrode, Phenols

INTRODUCTION

Due to their versatility and wide range of applications, activated carbons are widely used to remove various contaminants from liquid and gas phases. The performance characteristics of the activated carbons depend on their physicochemical properties, including the specific surface area, pore size distribution as well as the surface chemical composition. The nature and concentration of the surface functional groups responsible for the activated carbon properties may be modified by several methods. In general, the activated carbon modification techniques are categorized into three broad groups: chemical modification (acid treatment, base treatment, liquid oxidant treatment, ozone or other gases treatment, surfactant treatment, impregnation), physical modification (heat treatment, microwave) and biological modification (bioadsorption) [1,2]. The thermal modification of the activated carbon is generally at relatively low temperatures not exceeding the activation temperature (below 1,000 °C). Such a heat treatment leads to the destruction of the thermally unstable oxygen surface functional groups, but does not significantly affect the porous structure of the activated carbons nor change their crystalline structure [3].

The problem of the influence of the thermal treatment activated carbons at high temperatures in the range of 1,000-3,000 °C on their properties has long aroused interest [4-7]. Heat treatment enlarges crystallites of the activated carbon and makes them more ordered. In the case of other carbon materials, e.g., carbon black whose specific surface area is generally not too high and is mainly in the range of 50-200 $m^2 g^{-1}$, the heating effects are less visible (not too large a drop in the specific surface area), at high temperatures one can observe gradual graphitization. In the case of the activated carbon - the carbon materials with a well developed porosity (the specific surface areas are generally in the range of 1,000 to 2,000 $m^2 g^{-1}$, and can also achieve higher values), the annealing temperature as low as approx. 1,500 °C leads to a significant decrease in the surface area. After passing 1,900 °C this decline is dramatic (up to 10-20 $m^2 g^{-1}$).

In addition to be purely cognitive [5], the influence of the effects of annealing (especially the decrease in specific surface area) were also investigated, on the possibility of applying such activated carbons in the areas where they are most interesting for the carbon materials, for example, the capacitors of a double layer as the electrode material [8], in catalysis - the carrier of the metal catalyst [9], or in the adsorption from liquid or gaseous phase [10]. In the case of supercapacitors [8], the thermal treating of the activated carbon electrodes enhances the potential stability. For 6000 charging/discharging cycle times, the potential stability increases with the heat-treatment temperature increasing, achieving a fully positive effect starting from 1,500 °C. When using the activated carbon in the catalysis [9], for example, carbon annealed at 1,900 °C, the internal structure underwent as a result, a certainty of order, then was subjected to reactivation, e.g., steam at 760-885 °C to restore the former surface area. The resulting carbon turbostratic materials (with a more ordered internal structure) have superior properties as a catalyst carrier than the starting activated carbon (only washed away in water or deashed, e.g., by hydrochloric acid). In the latter case, the adsorption from the liquid phase was decreased with the increasing annealing temperature [10]. Generally, the annealed carbons, depending on the temperature and processing time, have greatly different modified properties (to varying degrees depending on the temperature): reduced surface area, increased electrical conductivity and a more

†To whom correspondence should be addressed.
E-mail: krzysztof.kusmierek@wat.edu.pl

orderly internal structure. At temperatures less than 1,900-2,000 °C, a decrease of the specific surface area [8,10] and micropore volume [5,8,10] is observed, and at higher temperatures the graphitization process is predominant [5,8]. Such a method (thermal treatment) allows the choice of the temperature and processing time to obtain a porous carbonaceous material with properties adapted to the requirements of the future use. When used in our study, the samples of the activated carbon were heat-treated at different temperatures as CPEs modifiers to assess the extent to which the altered properties will affect the usefulness in the electroanalysis.

The carbon paste electrode (CPE), whose main component is the paste made up of graphite powder and paraffin oil (Nujol), was placed in a cavity of the housing provided with electrical contacts, which played an important role in the electroanalysis [11,12]. It underwent various modifications, often consisting of the adding of a third component to the paste. Other researchers investigated several different modifiers, including siliceous materials, metal oxides and carbon materials. A significant proportion of them were nanomaterials. In most of the work only one type of modifier was used, changing only its proportion in relation to the graphite. Rarely compared in one paper, the CPEs were modified by the addition of the various materials.

Our aim was to evaluate the adsorption potential of the thermal modified activated carbon towards phenol (Ph), 4-chlorophenol (4-CP) and 2,4-dichlorophenol (2,4-DCP). The kinetic studies and adsorption isotherms of these compounds were reviewed and the results were analyzed by applying conventional theoretical models. The use of the non-modified and the thermal treated activated carbons in the preparation of the carbon paste electrodes for the detection of the phenols based on the differential pulse voltammetry was also investigated.

EXPERIMENTAL

1. Chemicals and Materials

The phenol, 4-chlorophenol, 2,4-dichlorophenol were purchased from Sigma-Aldrich (St Louis, MO, USA). The physicochemical properties and molecular structures of the selected compounds are given in Table 1. The graphite powder (diameter <45 μm) and high purity mineral oil (Nujol) used in the preparation of the carbon paste were obtained from Sigma-Aldrich and Fluka, respectively.

A commercial activated carbon R3-ex (Norit, The Netherlands) was demineralized with concentrated HF and HCl acids and the samples were heated in an argon atmosphere at 1,500 and 1,800 °C (at a constant heating rate of 15 °C min^{-1}). Details are described elsewhere [13,14]. Prior to use, the materials were oven dried at 120 °C to a constant weight and kept in a desiccator for further study.

The activated carbons to be tested were characterized texturally by means of nitrogen adsorption-desorption isotherms at 77.4 K measured on a Micromeritics ASAP 2010 volumetric adsorption analyzer (Norcross, GA, USA). The specific surface areas (S_{BET}) as well as the micropore (V_{mi}) and mesopore (V_{me}) volumes were calculated from the adsorption isotherms.

The thermal analyses of the test samples involved a Netzsch STA 449F3-Jupiter thermal analyzer. The samples were heated from 40 °C to 1,000 °C in Al_2O_3 crucibles under an air atmosphere with a flow rate of 50 cm^3 min^{-1}. The heating rate was 10 °C min^{-1}.

2. Adsorption Procedure

The batch adsorption experiments were carried out in Erlenmeyer flasks at a room temperature of 25 °C. In each experiment, 0.01 g of the activated carbon was first added to a 0.04 L solution of Ph, 4-CP or 2,4-DCP. The flasks were then agitated at a constant speed of 200 rpm. The concentration of the adsorbates in the aqueous phase was determined by using a UV-Vis spectrophotometer (Carry 3E, Varian, USA) at the wavelengths of 269, 278 and 281 nm, which correspond to the maximum absorption peaks of the Ph, 4-CP and 2,4-DCP, respectively. The calibration curves for the phenolic compounds were linear in the tested ranges (from 0.05 to 1.5 mmol L^{-1}) with correlation coefficients (R^2) better than 0.997. The equations for the regression line (n=3) were: y=1.377x+0.065 for phenol, y=1.411x+0.052 for 4-chlorophenol and y=1.673x+0,1807 for 2,4-dichlorophenol (where y is the absorbance and x is the concentration of the adsorbate).

Kinetic studies were conducted for initial adsorbate concentrations of 1.0 mmol L^{-1}. The amount of adsorption, q_t (mmol g^{-1}), at time t, was calculated according to the following equation:

$$q_t = \frac{(C_0 - C_t)V}{m} \quad (1)$$

where C_0 and C_t are the initial concentration and concentration at time t (mmol L^{-1}), V is the volume of the solution (L) and m is the mass of the activated carbon (g).

Adsorption isotherm experiments were conducted by adding 0.01 g of the activated carbon to 0.04 L of adsorbate solutions of different concentrations (0.5-2.0 mmol L^{-1}). The adsorption capacity q_e (mmol g^{-1}) of the adsorbent was calculated using the following equation:

Table 1. Physicochemical properties of the phenols

Compound	Chemical structure	Molecular weight	Molecular size (Å)	Solubility in water at 25 °C (g L^{-1})	pK_a
Phenol	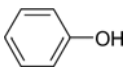	94.11	5.76×4.17	93	10.0
4-Chlorophenol	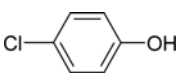	128.56	6.47×4.17	28	9.2
2,4-Dichlorophenol	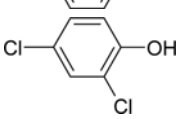	163.00	6.47×4.82	4.5	7.8

$$q_e = \frac{(C_0 - C_e)V}{m} \quad (2)$$

where C_e is the equilibrium concentration of the phenols (mmol L^{-1}) in the solution.

All the experiments were carried out in duplicate, and the average values were used for further calculations, the experimental error being around 4% (mean value).

3. Electrochemistry

The voltammetric measurements were carried out in a 0.04 L thermostated glass cell at room temperature, in a three-electrode configuration system. A carbon paste electrode was used as a working electrode. The reference electrode was a saturated calomel electrode and the counter electrode was a platinum wire. The differential pulse voltammetric measurements were performed in an Auto-Lab potentiostat/galvanostat (model PGSTAT 20, Eco Chemie B.V., Utrecht, The Netherlands) connected to a desktop computer and controlled by GPES 4.9 software. All the voltammograms were registered from 0 to +1.0 V at a sweep rate of 50 mV s^{-1}; the pulse height and width were set as 50 mV and 50 ms, respectively. The sampling time was 50 ms. The peak height was evaluated by the GPES software.

The fabrication of the carbon paste electrode and the modified carbon paste electrodes was as follows: the carbon paste electrode was prepared by thoroughly mixing graphite powder and paraffin oil in a mortar with pestle; the modified carbon paste electrodes were prepared in the same manner by precisely mixing weighed amounts (5 and 10% wt) of the activated carbon (AC-NM, AC1500 or AC1800) with graphite powder and paraffin oil. The mixture was kept at 25 °C for three days in a desiccator. After that, the paste was packed into the electrode cavity (2 mm) with Ø 3 mm. Before each use, the electrode surface was rubbed with a piece of paper until a smooth surface was observed.

RESULTS AND DISCUSSION

1. Adsorbents Characterization

Fig. 1 shows the adsorption-desorption isotherms of N_2 at 77 K on the non-modified activated carbon (AC-NM) as well as on the activated carbons heated at 1,500 °C (AC1500) and 1,800 °C (AC1800). The parameters characterizing the porous structure were calculated on the basis of the isotherms and are presented in Table 2. As can be seen, the thermal treatment of the AC-NM activated carbon gives the carbon samples a significantly decreased specific surface area as well as the micropore volumes. Similarly, one can observe a drop in the share of the micropore volume in the total volume of the micro- and mesopores. Also, changes in the overall crystallinity of the tested activated carbons were observed. The spacing d_{002} in the stacking structure of the aromatic layers calculated from the position of line (002) in the XRD patterns was 0.397, 0.383 and 0.377 nm for the AC-NM, AC1500 and AC1800 activated carbons, respectively [14]. The thermal treatment of the activated carbon brings a decrease in the d_{002} distance together with an increasing temperature, which improves the crystallinity, reduces the strain, and increases the crystallite sizes. Fig. 2 shows the results of the thermogravimetric analysis of all the tested activated carbons. The registered TG curves reveal the different temperatures at the beginning of the carbon combustion in an air atmosphere: 588, 630 and 656 °C for the AC-NM, AC1500 and AC1800 activated carbons, respectively. These differences result from the increasingly ordered structure of the carbons with the increasing temperature of its heating.

Table 2. Porous structure parameters obtained from nitrogen adsorption isotherms (77.4 K)

AC	S_{BET} ($m^2\ g^{-1}$)	V_{mi} ($cm^3\ g^{-1}$)	V_{me} ($cm^3\ g^{-1}$)	$V_{mi}/(V_{mi}+V_{me})$
AC-NM	1386	0.457	0.083	0.846
AC1500	967	0.293	0.103	0.740
AC1800	554	0.131	0.167	0.440

2. Adsorption Studies

The adsorption kinetic curves of the phenols on the AC-NM, AC1500 and AC1800 activated carbons are presented in Fig. 3. The adsorption equilibria of the Ph, 4-CP and 2,4-DCP were achieved

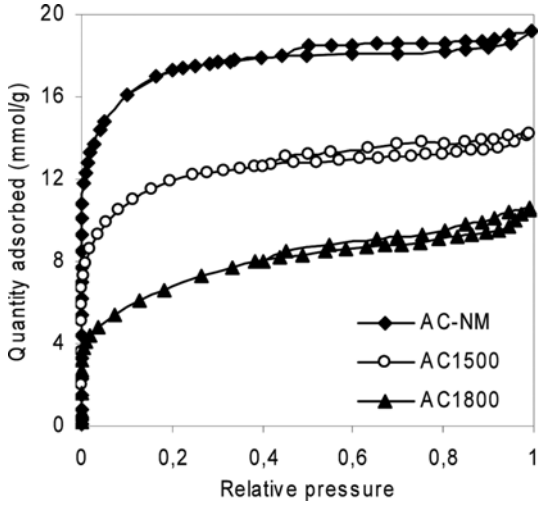

Fig. 1. Nitrogen adsorption-desorption isotherms at 77.4 K for AC-NM, AC1500 and AC1800 activated carbons.

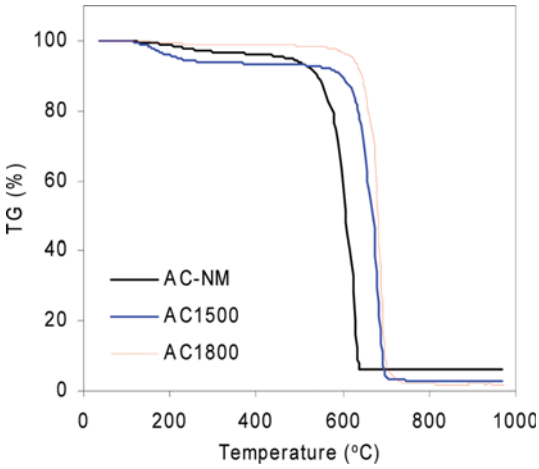

Fig. 2. Thermogravimetric measurements of the activated carbons: AC-NM, AC1500, AC1800.

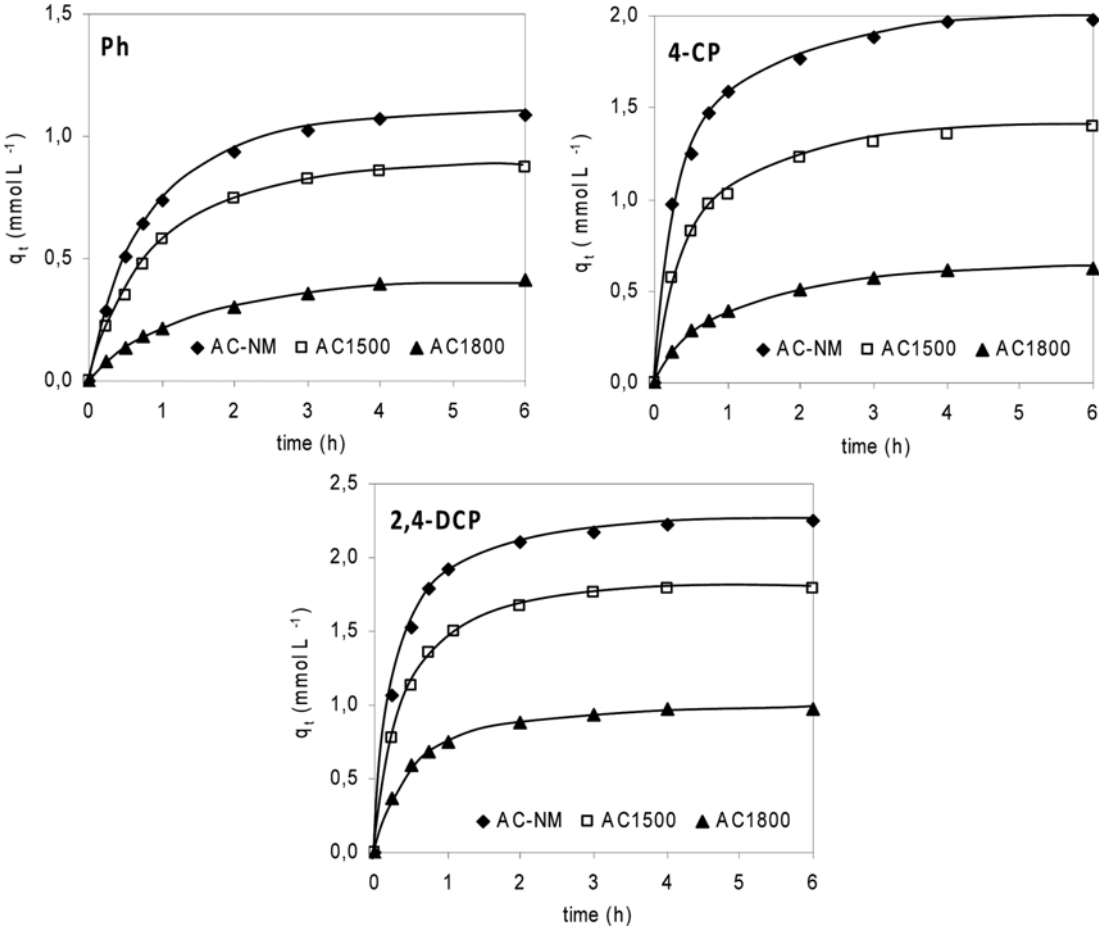

Fig. 3. Adsorption kinetics of the phenolic compounds on AC-NM, AC1500 and AC1800.

after about 4-5 h for all the absorbents. Two kinetic models, the pseudo-first order [15] and pseudo-second order [16], were used for the description of the experimental data. The pseudo-first order equation has a linear form:

$$\log(q_e - q_t) = \log q_e - \frac{k_1}{2.303}t \quad (3)$$

where k_1 is the pseudo-first order rate constant (h^{-1}). The values of k_1 were obtained from the intercept and the slope of the linear plot of $\log(q_e - q_t)$ vs. t.

The pseudo-second order kinetic model is expressed in linear form as:

$$\frac{t}{q_t} = \frac{1}{k_2 q_e^2} + \frac{1}{q_e}t \quad (4)$$

where k_2 is the pseudo-second order rate constant (g mmol^{-1} min^{-1}).

Table 3. The pseudo-first order and pseudo-second order kinetic parameters for phenol, 4-chlorophenol and 2,4-dichlorophenol adsorption on the activated carbons

Adsorbent	Adsorbate	$q_{e(EXP)}$	Pseudo-first order			Pseudo-second order		
			k_1	R^2	$q_{e(CAL)}$	k_2	R^2	$q_{e(CAL)}$
AC-NM	Ph	1.089	0.905	0.977	0.991	1.138	0.999	1.133
	4-CP	1.975	0.938	0.972	1.485	1.524	0.999	2.086
	2,4-DCP	2.245	1.027	0.964	1.636	1.705	0.999	2.297
AC1500	Ph	0.875	0.946	0.989	1.055	1.205	0.997	0.838
	4-CP	1.392	0.989	0.982	0.985	1.627	0.999	1.451
	2,4-DCP	1.802	1.078	0.938	1.093	1.967	0.999	1.822
AC1800	Ph	0.410	1.012	0.971	0.513	1.443	0.998	0.467
	4-CP	0.621	1.189	0.982	0.711	1.806	0.999	0.637
	2,4-DCP	0.980	1.274	0.967	0.791	2.310	0.998	1.031

The rate constants of the pseudo-second order adsorption (k_2) were calculated from the straight-line plots of t/q_t vs. t.

Table 3 presents the kinetic parameters for the adsorption of the phenolic compounds on the tested activated carbons. The correlation coefficients for the pseudo-first order kinetic model are relatively low, whereas the R^2 values for the pseudo-second order kinetic model are higher than 0.997. Furthermore, in the pseudo-second order kinetic model the calculated $q_{e(CAL)}$ are very close to the experimental $q_{e(EXP)}$ values. This indicates that the adsorption system belongs to the pseudo-second order kinetic model. The results revealed that the increasing of the degree of the chlorine substitution on the phenol ring increased the adsorption rate of the phenolic compounds on all the activated carbons. The adsorption rate increased in the order: phenol<4-chlorophenol<2,4-dichlorophenol. Similar results were reported by Tseng et al. [17] for the phenol adsorption on the activated carbon derived from pistachio shells, and by Wu et al. [18] for the adsorption on the activated carbon with an average particle size of 285 and 505 μm. On the other hand, the same authors [18] found that the adsorption kinetics on the activated carbon with an average particle size of 715 μm was 4-CP< Ph<2,4-DCP, while on the AC having the largest particles (1,015 μm) followed the sequence 4-CP<2,4-DCP<Ph. Liu et al. [19] described that the k_2 values for the adsorption on the activated carbon fibers follow the order of phenol<2,4-DCP≈4-CP. Recently, Tseng et al. [20] revealed that the values of the pseudo-first order adsorption rates (k_1) on the microporous activated carbons from betel trunk increase in the order Ph<4-CP<2,4-DCP, and the values of the k_2 followed the sequence 4-CP<Ph<2,4-DCP. The 4-CP was adsorbed faster than Ph onto activated carbon obtained from lignocellulosic material [21] and activated carbon nanotubes [22]. On the other hand, on the commercial AC Sigma-Aldrich and unmodified carbon nanotubes the order was reversed (Ph>4-CP) [22]. Garba and Rahim [23] as well as Kuśmierek [24] found that the 2,4-DCP was adsorbed faster than 4-CP on the activated carbon from an agricultural waste and powdered activated carbon, respectively. The adsorption rate of the phenolic compounds on the activated carbon prepared from jackfruit peel [25] and the carbon-coated monolith [26] increased in the order: 2,4-DCP<4-CP< Ph. These examples suggest that there is no clear relationship between the chemical structure of the adsorbates (e.g. the chlorine substitution on the aromatic ring, molecular size) and their adsorption kinetics on the activated carbons.

All the adsorbates were adsorbed faster on the AC1800 than on the AC1500 and non-modified activated carbon. The k_2 values of the Ph, 4-CP and 2,4-DCP increased in the order: AC-NM< AC1500<AC1800. Lorenc-Grabowska et al. [27] reported that the

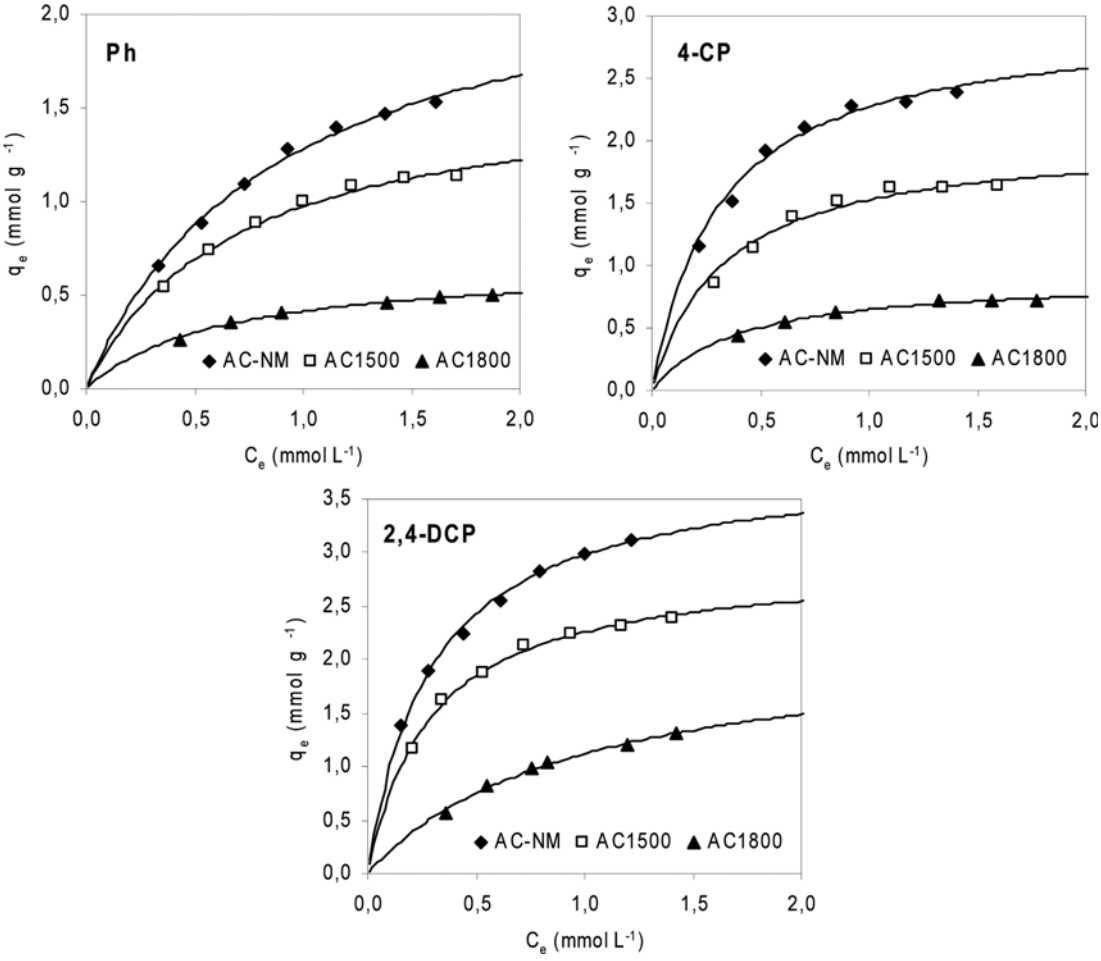

Fig. 4. Adsorption isotherms of phenol, 4-chlorophenol and 2,4-dichlorophenol on tested activated carbons.

time required to reach equilibrium is usually related to the volume of the macro- and mesopores that play the role of transporting arteries. As can be seen in Table 2, the increase in the mesopore volumes of the activated carbons corresponds to their faster adsorption toward the phenolic compounds.

The adsorption isotherms of the phenolic compounds on the AC-NM, AC1500 and AC1800 activated carbons are shown in Fig. 4. Two isotherm models (Langmuir and Freundlich) were used to test the fitting of the experimental data. The linear form of the Langmuir [28] isotherm is described by:

$$\frac{C_e}{q_e} = \frac{1}{q_m} C_e + \frac{1}{q_m b} \quad (5)$$

where q_m [mmol g^{-1}] is the maximum adsorption capacity and b [L $mmol^{-1}$] is the constant related to the free energy of the adsorption. To obtain the rate constants and correlation coefficients, the straight-line plots of C_e/q_e vs. C_e were tested.

The linear form of the Freundlich [29] isotherm is given by the following equation:

$$\ln q_e = \ln K_F + \frac{1}{n} \ln C_e \quad (6)$$

where K_F (mmol g^{-1})·(L $mmol^{-1}$)$^{1/n}$, and n are the Freundlich equation constants which relate to the adsorption capacity and the adsorption intensity of the adsorbent. The values of K_F and n were determined from the intercept and slope from plot of $\ln C_e$ vs. $\ln q_e$. The calculated adsorption constants as well as the correlation coefficients are presented in Table 4.

The R^2 values (>0.99) show that the equilibrium data obtained for all the adsorbents (and all of the adsorbates) were well represented by the Langmuir isotherm compared to the Freundlich equation. The fact that the experimental data fitted better to the Langmuir isotherm may be due to the homogeneous distribution of the active sites on the surface of the activated carbons, since the Langmuir

Table 4. Parameters of the Langmuir and Freundlich adsorption isotherm models for the Ph, 4-CP and 2,4-DCP

Adsorbent	Adsorbate	Langmuir			Freundlich		
		q_m	b	R^2	K_F	n	R^2
AC-NM	Ph	2.408	1.136	0.994	1.251	1.817	0.979
	4-CP	2.976	3.221	0.991	2.283	2.533	0.925
	2,4-DCP	3.856	3.407	0.999	3.014	2.547	0.985
AC1500	Ph	1.637	1.462	0.991	0.947	2.064	0.960
	4-CP	2.023	3.063	0.991	1.504	2.656	0.912
	2,4-DCP	2.910	3.474	0.998	2.262	2.712	0.938
AC1800	Ph	0.668	1.616	0.995	0.402	2.262	0.952
	4-CP	1.114	2.496	0.996	0.627	2.917	0.947
	2,4-DCP	2.190	1.039	0.991	1.108	3.536	0.973

Table 5. Comparison of phenols adsorption on various activated carbons

Adsorbent	S_{BET} $m^2 g^{-1}$	Adsorption capacity, q_m (mg g^{-1})			Ref.
		Ph	4-CP	2,4-DCP	
AC-NM	1390	226.6	382.6	628.5	This study
AC1500	970	154.0	260.1	474.3	This study
AC1800	530	62.9	143.2	357.0	This study
Commercial AC Prolabo	929	250.0	323.0	370.0	[32]
Commercial AC Merck	760	148.6	336.9	336.9	[35]
Activated carbon fibers	920	102.5	242.4	367.4	[19]
AC from jackfruit peel	-	145.0	277.7	400.0	[25]
Carbon-coated monolith	470	65.8	114.9	156.3	[26]
Commercial AC Sigma-Aldrich	1187	283.3	280.0	-	[22]
AC from lignocellulosic material	300	55.6	200.0	-	[21]
AC 800SP-NH_3	385	316.5	330.2	-	[34]
AC from an agricultural waste	1086	-	347.5	380.8	[23]
Commercial AC (Cumming & Sons)	945	-	319.0	467.0	[36]
AC from PET (PET-25C)	1117	276	-	-	[27]
Commercial L2S Ceca AC	925	-	256.7	-	[37]
Modified R3ex Norit AC	1530	-	386.2	-	[37]
Modified AC (AP42)	853	-	-	339.0	[31]

equation assumes the homogeneity of the surface.

The phenolic compounds were preferably adsorbed on the non-modified activated carbon, followed by the AC1500, and the worst on the AC1800 activated carbon. The q_m and K_F values obtained for all the activated carbons decreased in the order AC-NM> AC1500>AC1800. This fact indicated that the adsorption on the activated carbons used in this study was dependent on the surface area: the adsorption capacity decreased in the decrease of the S_{BET} of the ACs. The values of the Freundlich constant n were greater than one, indicating a favorable adsorption of the phenolic compounds by all the adsorbents.

It is well known, from previous works [30-32], that the adsorption of the phenols is associated with their physicochemical properties, including the molecular weight and size, hydrophobicity, solubility and pK_a. As can be seen in Table 4, the adsorption efficiency increased in the order phenol<4-chlorophenol<2,4-dichlorophenol, which was correlated with respective increase in the molecular weight and size, as well as the decrease in the solubility of the adsorbates (Table 1). The adsorption increased also with a decrease in the pK_a values of the phenols; however, in this case, the pK_a does not have a significant role in the adsorption because all of the experiments were conducted in water (at a natural pH) where the adsorbates existed predominantly in non-dissociated forms. Similar results, the increased adsorption efficiency of the phenols with the increasing of the degree of the chlorine substitution on the phenol ring, were reported by other authors [19,21,23-26,31-36].

Table 5 compares the adsorption capacities of the Ph, 4-CP and 2,4-DCP on the AC-NM, AC1500 and AC1800 activated carbons obtained in this work with other studies. For comparison, only the Langmuir maximum adsorption capacities q_m were used. In addition, all the units have been standardized and converted to mg g^{-1}.

3. Electrochemical Studies

The results from the DPV registered for the 0.5 mmol L^{-1} solutions of the Ph, 4-CP and 2,4-DCP (in 0.1 mol L^{-1} sodium sulfate) using a carbon paste electrode containing 5% or 10% by mass of the tested activated carbons are presented in Table 6. The differential pulse voltammograms of the Ph, 4-CP and 2,4-DCP using a CPE containing 10% of the modifiers are presented in Fig. 5.

The peak potential of the Ph, 4-CP and 2,4-DCP was 0.73-0.74, 0.75-0.76 and 0.78-0.79 V, respectively. In any case, the signal observed at 10% modifier content was about two-times higher as compared to the electrodes containing 5% of the additives and several times higher than that of the bare electrode. The peak current increased in the order phenol<4-chlorophenol<2,4-dichlorophenol for all of the CPEs. The same sequence was observed in the adsorption rate and the adsorption effectiveness on all the activated carbons. This suggests that the electrochemical oxidation of the phenolic compounds at the modified carbon paste electrodes used in these studies is controlled by adsorption. Moreover, the higher peak currents were observed for the electrodes modified with the activated carbons of a greater specific surface area (AC1800<AC1500 <AC-NM). Similar results were described for the detection of 4-chlorophenol [37] and 2,4-dichlorophenoxyacetic acid [38]. The authors reported [37,38] that the sensitivity of the methods was correlated with the type of the modifier - the analytical signal was increased with the adsorption capacity and the specific surface area of the materials used. Nevertheless, for the preparation of the electrodes the authors used various carbonaceous materials including activated carbons and carbon black [37] as well as activated carbons, carbon blacks and carbon molecular sieves [38]. Also, the activated carbons used were derived from the different precursors and they differed in the manufacturing and activation method. Therefore, a conclusive relationship between the electroanalytical signal and the specific surface area of the CPE modifiers was not possible. In this work, as a modifier only one AC (modified at a high temperatures) was used. It was found that the intensity of the signal increased linearly with the increase of the specific surface area of the modifiers (Fig. 6). The results confirmed clearly the

Table 6. Peak currents and potentials determined from DPV curves for carbon paste electrodes modified by adding various quantity of thermal activated carbon materials

CPE modifier	Modifier content % wt	Ph	4-CP	2,4-DCP
		I (μA)	I (μA)	I (μA)
Bare CPE	-	0.24	0.31	0.40
AC-NM	5	0.81	1.43	1.82
	10	1.32	2.01	2.45
AC1500	5	0.64	1.05	1.57
	10	1.08	1.69	2.16
AC1800	5	0.39	0.57	0.95
	10	0.72	1.12	1.84

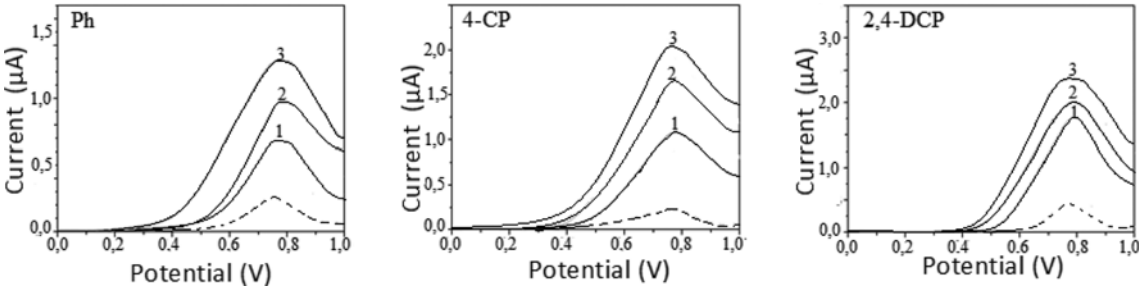

Fig. 5. The DPV curves registered for 0.5 mmol L^{-1} phenol, 4-CP and 2,4-DCP in 0.1 mol L^{-1} Na_2SO_4 solutions using carbon paste electrodes containing 10% by mass of tested materials. Modifiers: 1 - AC-NM, 2 - AC1500, 3 - AC1800, dashed line - unmodified carbon paste electrode.

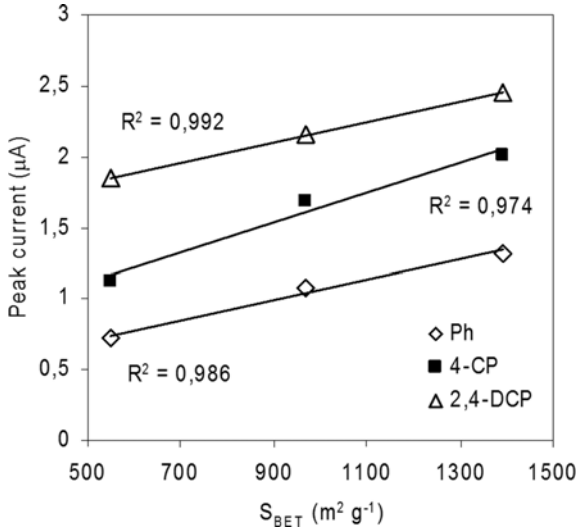

Fig. 6. The plots of the peak currents from the DPV analysis versus the specific surface area of the carbon paste electrode modifiers.

direct relationship between the analytical signal and the specific surface area of the modifier used for the preparation of the CPE.

The limits of detection and quantitation were calculated using the equations LOD=3σ/*a* and LOQ=6σ/*a*, respectively, where σ is a standard deviation of the blank signal and *a* is a slope of the calibration curve. In each case, nine blank measurements were carried out. The calibration curves were constructed by plotting the peak current vs. the adsorbates concentration and the curves were fitted by least squares linear regression analysis. The calibration ranges were 0.05-0.5 mmol L^{-1} for all the compounds. The equations for the linear regression lines, regression coefficients as well as the LOD and LOQ are shown in Table 7. Both the LOD and LOQ decreased with the increasing of the S_{BET} of the modifiers. Compared to the non-modified electrode, all the new paste electrodes showed a significantly greater sensitivity for the detection of the phenols.

The lowest LOD and LOQ were observed for the carbon paste electrode modified with the AC-NM. The LOD of the 4-CP was found to be 0.032 μmol L^{-1}, and was comparable with the montmorillonite-modified carbon paste electrode reported by Yang et al. (0.02 μmol L^{-1}) [39], and much better than that of the CPEs modified with the mesoporous silica SBA-15 (1.4 μmol L^{-1}) and SBA-15-NH_2 (0.4 μmol L^{-1}) [40].

CONCLUSIONS

The applied activated carbons showed significant differences in the porous structure and in the crystalline structure. The thermal treatment gave a decreasing specific surface area as well as the micropore volume, and an increasing order of crystalline structure along with an increasing temperature of heating. The adsorption of the phenol, 4-chlorophenol and 2,4-dichlorophenol from the aqueous solutions on the non-modified activated carbon and activated carbons heated at 1,500 and 1,800 °C was studied. The adsorption kinetics was better represented by the pseudo-second order model. The results showed that the increasing of the degree of the chlorine substitution on the phenol ring increased the adsorption rate of the phenolic compounds on all the activated carbons. The adsorption isotherms of the phenols were analyzed by using the Freundlich and Langmuir models. The experimental data received were well described by the Langmuir isotherm equation. The adsorption efficiency increased in the order: phenol<4-chlorophenol<2,4-dichlorophenol. The adsorption of the phenols was dependent on the porosity of the activated carbons: the adsorption rate increased with the increase in the mesopore volumes of the activated carbons, while the adsorption capacity increased with the increase of the S_{BET} of the ACs. The thermally treated activated

Table 7. Linearity results for the CPEs containing 10% wt of the modifier (n=3)

CPE modifier	Linear regression equation y=ax+b	R^2	LOD μmol L^{-1}	LOQ μmol L^{-1}
		Ph		
Bare CPE	y=0.57x+0.112	0.978	0.318	0.635
AC-NM	y=4.31x+0.359	0.985	0.042	0.084
AC1500	y=3.68x+0.336	0.998	0.049	0.098
AC1800	y=3.26x+0.223	0.999	0.056	0.113
		4-CP		
Bare CPE	y=0.42x+0.106	0.999	0.259	0.518
AC-NM	y=3.42x+0.311	0.999	0.032	0.064
AC1500	y=2.95x+0.229	0.998	0.037	0.073
AC1800	y=2.01x+0.126	0.999	0.054	0.107
		2,4-DCP		
Bare CPE	y=0.39x+0.046	0.998	0.138	0.278
AC-NM	y=2.43x+0.281	0.993	0.021	0.042
AC1500	y=2.21x+0.011	0.999	0.025	0.049
AC1800	y=1.44x+0.028	0.999	0.038	0.075

carbons were also used for the modification of the carbon paste electrodes for the detection of the phenols based on the differential pulse voltammetry. The peak current increased in the same sequence as the adsorption rate and the equilibrium (phenol<4-chlorophenol<2,4-dichlorophenol), suggesting that the electrochemical oxidation of the phenols at the modified CPEs used in these studies was controlled by adsorption. The sensitivity of the methods was correlated with the porosity of the activated carbons. The intensity of the signal increased linearly with the increase of the specific surface area of the modifiers. Compared to the non-modified electrode, all the new paste electrodes showed a significantly greater sensitivity for the detection of the phenols.

LIST OF SYMBOLS

2,4-DCP : 2,4-dichlorophenol
4-CP : 4-chlorophenol
AC1500 : activated carbon heated at 1,500 °C
AC1800 : activated carbon heated at 1,800 °C
AC-NM : non-modified activated carbon
b : Langmuir constant related to the free energy of the adsorption [L $mmol^{-1}$]
C_0 : initial concentration of the adsorbate in solution [mmol L^{-1}]
C_e : equilibrium concentration of the adsorbate in solution [mmol L^{-1}]
CPE : carbon paste electrode
C_t : concentration of the adsorbate at time t [mmol L^{-1}]
DPV : differential pulse voltammetry
k_1 : pseudo-first order rate constant [h^{-1}]
k_2 : pseudo-second order rate constant [g $mmol^{-1}$ min^{-1}]
K_F : Freundlich constant indicative of the relative adsorption capacity of the adsorbent (mmol/g)·$(L/mmol)^{1/n}$
I : peak current [μA]
LOD : limit of detection
LOQ : limit of quantitation
m : mass of the adsorbent [g]
n : Freundlich constant indicative of the intensity of the adsorption
Ph : phenol
q_e : amount of solute adsorbed per unit weight of adsorbent at equilibrium [mmol/g]
q_m : Langmuir maximum adsorption capacity [mmol g^{-1}]
q_t : amount of solute adsorbed at time t [mmol g^{-1}]
R^2 : correlation coefficient
S_{BET} : Brunauer-Emmett-Teller surface area [m^2 g^{-1}]
S_{me} : mesopore surface area [m^2 g^{-1}]
V : volume of the solution [L]
V_{me} : mesopore volume [cm^3 g^{-1}]
V_{mi} : micropore volume [cm^3 g^{-1}]

REFERENCES

1. C. Y. Yin, M. K. Aroua and W. M. A. W. Daud, *Sep. Purif. Technol.*, **52**, 403 (2007).
2. A. Bhatnagar, W. Hogland, M. Marques and M. Sillanpää, *Chem. Eng. J.*, **219**, 499 (2013).
3. H. Grajek, A. Świątkowski, Z. Witkiewicz, M. Pakuła and S. Biniak, *Ads. Sci. Technol.*, **19**, 565 (2001).
4. R. E. Franklin, *Proc. of the Royal Society of London, Series A, Mathematical and Physical Sciences*, **209**, 196 (1951).
5. M. M. Dubinin, *Thermal treatment and microporous structure of carbonaceous adsorbents*, Proc. of the Fifth Conference on Carbon, vol. 1, Pennsylvania State University, Pergamon Press Inc., New York (1962).
6. F. G. Emmerich**,** *Carbon*, **33**(12), 1709 (1995).
7. M. Inagaki, M. Toyoda and T. Tsumura, *RSC Adv.*, **4**, 41411 (2014).
8. G. Sun, C. Wang, L. Zhan, W. Qiao, X. Liang and L. Ling, *J. Mater. Sci. Eng.*, **2**, 41 (2008).
9. M. Bonarowska, W. Raróg-Pilecka and Z. Karpiński, *Catal. Today*, **169**, 223 (2011).
10. A. Świątkowski, A. Deryło-Marczewska, J. Goworek and S. Błażewicz, *Appl. Surf. Sci.*, **236**, 313 (2004).
11. I. Svancara, K. Vytras, K. Kalcher, A. Walcarius and J. Wang, *Electroanalysis*, **21**, 7 (2009).
12. I. Svancara, K. Kalcher, A. Walcarius and K. Vytras, *Electroanalysis with carbon paste electrodes*, CRC Press, Taylor & Francis Group, Boca Raton (2012).
13. S. Błażewicz, A. Świątkowski and B. J. Trznadel, *Carbon*, **37**, 693 (1999).
14. S. Biniak, M. Pakuła, A. Świątkowski, M. Bystrzejewski and S. Błażewicz, *J. Mater. Res.*, **25**(8), 1617 (2010).
15. S. Lagergren, *Vetenskapsakad. Handl.*, **24**, 1 (1898).
16. Y. S. Ho and G. McKay, *Process Biochem.*, **34**, 451 (1999).
17. R. L. Tseng, K. T. Wu, F. C. Wu and R. S. Juang, *J. Environ. Manage.*, **91**, 2208 (2010).
18. F. C. Wu, R. L. Tseng, S. C. Huang and R. S. Juang, *Chem. Eng. J.*, **151**, 1 (2009).
19. Q. S. Liu, T. Zheng, P. Wang, J. P. Jiang and N. Li, *Chem. Eng. J.*, **157**, 348 (2010).
20. R. L. Tseng, P. H. Wu, F. C. Wu and R. S. Juang, *Chem. Eng. J.*, **237**, 153 (2014).
21. N. G. Rincon-Silva, J. C. Moreno-Pirajan and L. Giraldo, *Adsorption*, **22**, 33 (2016).
22. P. Strachowski and M. Bystrzejewski, *Colloids Surf., A*, **467**, 113 (2015).
23. Z. N. Garba and A. A. Rahim, *Process Saf. Environ.*, **102**, 54 (2016).
24. K. Kuśmierek, *Reac. Kinet. Mech. Cat.*, **119**, 19 (2016).
25. S. Jain and R. V. Jayaram, *Sep. Sci. Technol.*, **42**, 2019 (2007).
26. Y. P. Teoh, M. A. Khan, T. S. Y. Choong, L. C. Abdullah and S. Hosseini, *Desalin. Water Treat.*, **54**, 393 (2015).
27. E. Lorenc-Grabowska, M. A. Diez and G. Gryglewicz, *J. Colloid Interface Sci.*, **469**, 205 (2016).
28. I. Langmuir, *J. Am. Chem. Soc.*, **38**, 2221 (1916).
29. H. M. F. Freundlich, *Z. Phys. Chem.*, **57**, 385 (1906).
30. A. Dąbrowski, P. Podkościelny, Z. Hubicki and M. Barczak, *Chemosphere*, **58**, 1049 (2005).
31. A. A. M. Daifullah and B. S. Girgis, *Water Res.*, **32**, 1169 (1998).
32. O. Hamdaoui and E. Naffrechoux, *J. Hazard. Mater.*, **147**, 381 (2007).
33. M. W. Jung, K. H. Ahn, Y. Lee, K. P. Kim, J. S. Rhee, J. T. Park and K. J. Paeng, *Microchem. J.*, **70**, 123 (2001).
34. Z. Zhang, X. Feng, X. X. Yue, F. Q. An, W. X. Zhou, J. F. Gao, T. P.

Hu and C. C. Wei, *Korean J. Chem. Eng.*, **32**(8), 1564 (2015).
35. M. Carmona, M. T. Garcia, A. Carnicer, M. Madrid and J. F. Rodriguez, *J. Chem. Technol. Biotechnol.*, **89**(11), 1660 (2014).
36. G. S. M. Hossain and R. G. McLaughlan, *Environ. Technol.*, **33**, 1839 (2012).
37. K. Kuśmierek, M. Sankowska, K. Skrzypczyńska and A. Świątkowski, *J. Colloid Interface Sci.*, **446**, 91 (2015).
38. K. Skrzypczyńska, K. Kuśmierek and A. Świątkowski, *J. Electroanal. Chem.*, **766**, 8 (2016).
39. H. Yang, X. Zheng, W. Huang and K. Wu, *Colloids Surf., B,* **65**, 281 (2008).
40. A. Deryło-Marczewska, M. Zienkiewicz-Strzałka, K. Skrzypczyńska, A. Świątkowski and K. Kuśmierek, *Adsorption*, **22**, 801 (2016).